Patterns of Craniofacial Size and Shape Variation from Medieval to Contemporary Human Populations

Anna Walczak[1*], Sylwia Łukasik[1], Antonio Profico[2], Jacek Tomczyk[3], Marta Krenz-Niedbała[1]

[1] Institute of Human Biology and Evolution, Faculty of Biology, Adam Mickiewicz University in Poznan, Uniwersytetu Poznańskiego 6, 61-614, Poznan, Poland

[2] Department of Biology, University of Pisa, Pisa 56127, Italy

[3] Institute of Biological Sciences, Cardinal Stefan Wyszyński University, Warsaw, Poland

[*]Corresponding author, walczak.anna@amu.edu.pl, +48 618295727

Supporting Information

This document contains the following supporting information, supplementing the discussion and results presented in the article “Patterns of Craniofacial Size and Shape Variation from Medieval to Contemporary Human Populations”:

- Supplementary Table S1 – Parental ancestry from New Mexico sample.
- Supplementary Table S2 – Definitions of landmarks used in analysis of the cranium
- Supplementary Text S1 – Description of PC3-PC5
- Supplementary Figure S1 – Shape variations described by PPC3, PC4, PC5 arranged in rows respectively. Average shape warped along each PCs maximal and minimal values (magenta and green, respectively)
- Supplementary Figure S2 – Surface warping built along PC3, PC4 and PC5 maximal and minimum values
- Supplementary Table S3 – Comparison of the PCA results in size and shape and in pure shape environment
- Supplementary Figure S3 – PCA plots for the first and third components a. in size-shape space. b. in pure shape space. Different samples are presented with three different colors, and sex is presented with symbols

Table S1 Parental ancestry from New Mexico sample.

	Number of individuals
Both parents born in the USA	199
One parent born in the USA, one parent unknown	8
One parent born in the USA, one parent born outside the USA	4
Both parents unknown	16
Both parents born outside the USA	0

Table S2 Definitions of landmarks used in analysis of the cranium.

No.	Name	Definition	Author
1	*Bregma*	The point of intersection between the sagittal and coronal sutures	Nikita (2016)
2	*Glabella*	The most anteriorly projecting point on the midsagittal plane, located between the superciliary arches	Nikita (2016)
3	*Nasion*	The point of intersection of the frontonasal and the internasal suture	Nikita (2016)
4	*Nasospinale*	The point of intersection between the midsagittal plane and a line tangent to the most inferior points on the margin of the nasal aperture	Nikita (2016)
5	*Alveolare*	The inferiormost point of the alveolar border in the midsagittal plane	Nikita (2016)
6-7	*Porion*	The superiormost point on the margin of the external auditory meatus	Nikita (2016)
8-9	*Stephanion*	The point of intersection between the coronal suture and the temporal line	Nikita (2016)
10-11	*Frontotemporale*	The point on the superior temporal line, lying at the base of the zygomatic process of the frontal bone	Nikita (2016)
12-13	*Supraorbitale*	The most superior point on the superior orbital margin	Toneva et al. (2022)
14-15	*Frontomalare temporale*	The lateralmost point of the frontozygomatic suture	Nikita (2016)
16-17	*Frontomalare orbitale*	The point of intersection between the frontozygomatic suture and the inner orbital rim	Nikita (2016)
18-19	*Maxillofrontale*	The point of intersection between the inner orbital margin and the frontomaxillary suture	Nikita (2016)
20-21	*Ectoconchion*	The point on the lateral orbital margin where an axis parallel to the superior orbital margin divides the orbit into two equal halves	Nikita (2016)
22-23	*Orbitale*	The most superior point on the inferior orbital margin	Martin and Saller (1928)
24-25	*Jugalia*	The points at the deepest curvature between the frontal and the temporal processes of the zygomatic bones	Nikita (2016)
26-27	Infraorbitale	The most superior point on the margin of the infraorbital foramen	Toneva et al. (2022)
28-29	*Alare*	The lateralmost point on the margin of the nasal aperture	Nikita (2016)
30-31	*Nariale*	The inferiormost point on the margin of the nasal aperture	Nikita (2016)
32-33	*Zygomaxillare*	The most inferior point on the zygomaticomaxillary suture	Martin and Saller (1928)

34-35	Canine	The uppermost point on the alveolar socket of the canine tooth	Defined by the author for this study.
36-37	Posterior maxilla	The most posterior point on the alveolar ridge of the maxilla	Defined by the author for this study.

Note:

Paired numbers indicate landmarks applied on the left and right side. Landmarks labeled "Defined by the author for this study" were determined based on careful inspection of the bone surfaces and designed to ensure comprehensive spatial coverage and patch stability for the geometric morphometric analysis.

Supplementary Text S1 Description of PC3-PC5

PC3 reflects proportional differences between the midface and upper facial regions, as well as changes in their relative widths. Morphology ranges from a narrower midface with a broader upper face and frontal bone to an expanded midface with a relatively narrower frontal bone. At higher PC3 values, midfacial contraction becomes more uniform, while the broadening of upper elements results from expansion in the lateral regions, including the upper orbits, where expansion proceeds from the central portion. In the frontal bone, expansion is pronounced, though in the forehead area; it is largely restricted to its frontal aspects, with the glabellar region and supraorbital margin becoming more expanded and prominent (Fig. S1 and S2). PC4 describes a shift from a longer to a shorter cranial morphology, accompanied by contrasting responses to the upper and midfacial structures. At the lower end of this axis, the maxilla, zygomatic bone, and the medial-to-lateral segment of the superior orbital rim contract strongly, while the mid- to medial upper orbit, glabellar region, and frontal squama expand. This combination produces a cranium that appears shorter but broader in its upper parts, with the opposite pattern occurring at the other extreme (Fig. S1 and S2). PC5 captures the effect of a broader upper facial skeleton, achieved through expansion of the lateral orbital regions and the lateral frontal bone. The midface contracts overall, although several localized areas, such as the lower portion of the piriform aperture and the central regions of the orbits, show distinct expansion.

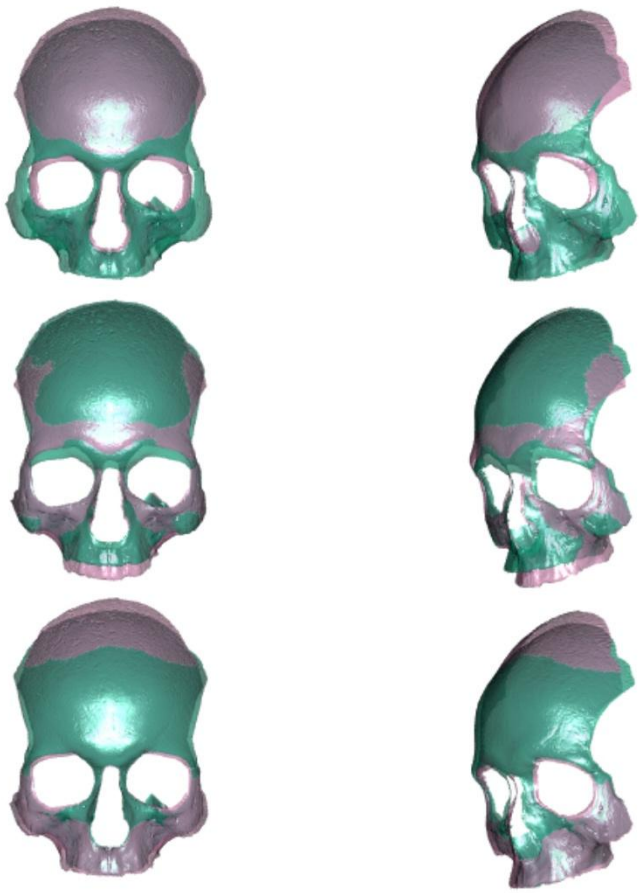

Fig. S1 Shape variations described by PPC3, PC4, PC5 arranged in rows respectively. Average shape warped along each PCs maximal and minimal values (magenta and green, respectively).

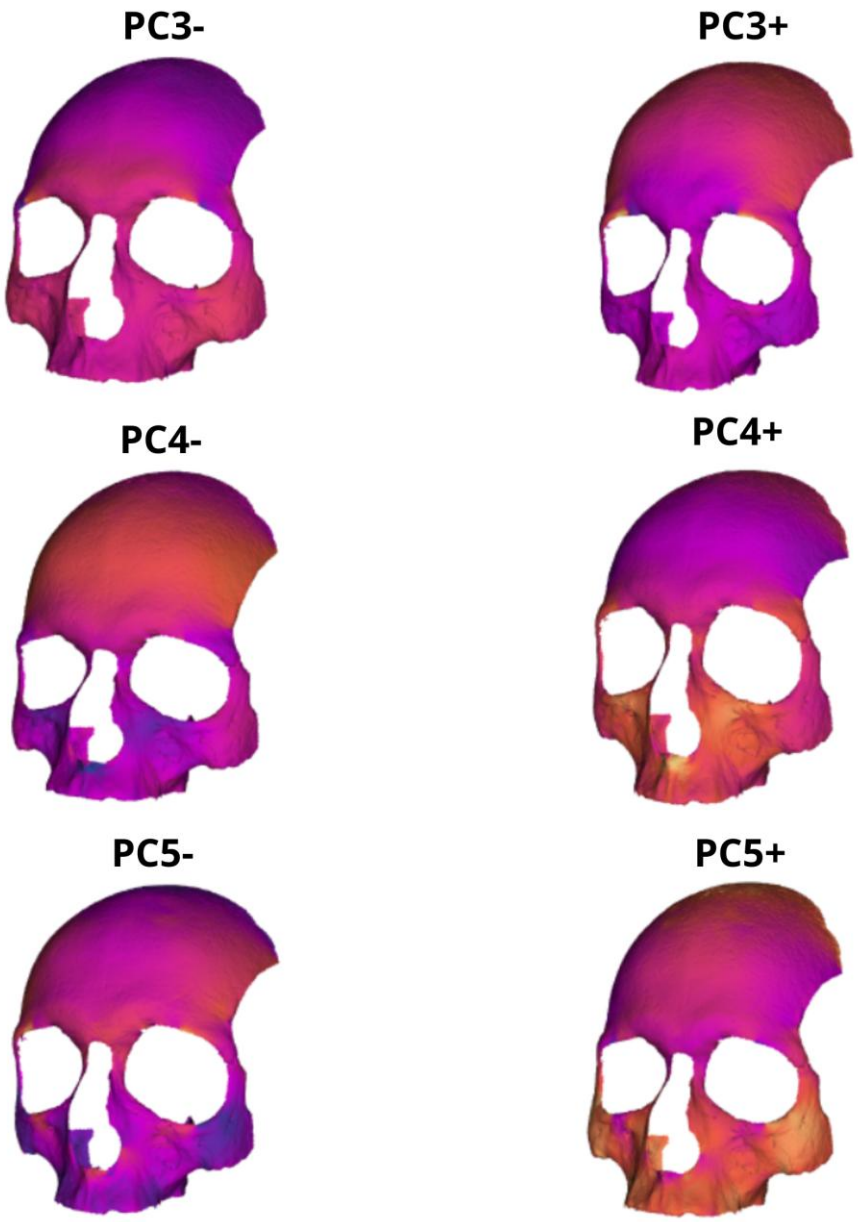

Fig. S2 Surface warping built along PC3, PC4 and PC5 maximal and minimum values.

Table S3 Comparison of the PCA results in size and shape and in pure shape environment.

	Shape		Size and shape	
	% variance explained	p-value	% variance explained	p-value
Sex	12.56	0.001	2.01	0.001
Sample	20.06	0.001	16.24	0.001
Age	6.11	0.001	4.04	0.001

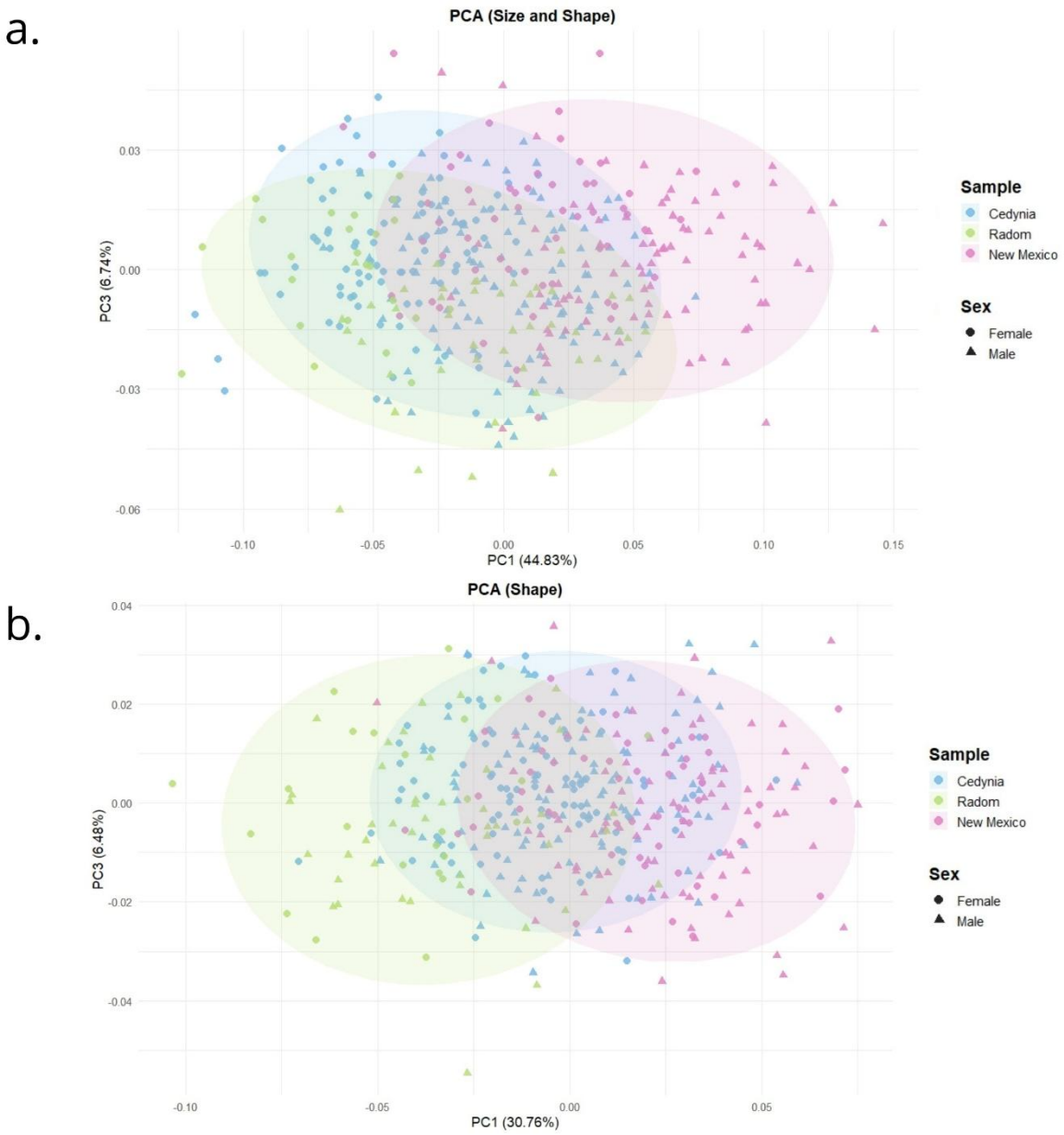

Fig. S3 PCA plots for the first and third components a. in size-shape space. b. in pure shape space. Different samples are presented with three different colors, and sex is presented with symbols.

References:

Martin, R., and K. Saller. 1928. “Lehrbuch Der Anthropologie. Band 2: Kraniologie.” *Osteologie. Jena: Gustav Fischer Verlag*.

Nikita, Efthymia. 2016. *Osteoarchaeology: A Guide to the Macroscopic Study of Human Skeletal Remains*. Academic Press.

Toneva, Diana, Silviya Nikolova, Elena Tasheva-Terzieva, Dora Zlatareva, and Nikolai Lazarov. 2022. “A Geometric Morphometric Study on Sexual Dimorphism in Viscerocranium.” *Biology* 11 (9): 1333.